

# Synthesis and characterization of cationic and zwitterionic allyl zirconium complexes derived from trimethylenemethane (TMM) cyclopentadienylzirconium acetamidinates

Denis A. Kissounko, James C. Fettinger, Lawrence R. Sita\*

Department of Chemistry and Biochemistry, University of Maryland, College Park, MD 20742, USA

Received 6 March 2003; received in revised form 1 April 2003; accepted 17 April 2003

## Abstract

Protonation of the trimethylenemethane derivatives,  $\text{Cp}^*\text{Zr}(\sigma^2, \pi\text{-C}_4\text{H}_6)[\text{N}(\text{R}^1)\text{C}(\text{Me})\text{N}(\text{R}^2)]$  (**1a**:  $\text{R}^1 = \text{R}^2 = i\text{-Pr}$  and **1b**:  $\text{R}^1 = \text{Et}$ ,  $\text{R}^2 = t\text{-Bu}$ ) ( $\text{Cp}^* = \eta^5\text{-C}_5\text{Me}_5$ ), by  $[\text{PhNMe}_2\text{H}][\text{B}(\text{C}_6\text{F}_5)_4]$  in chlorobenzene at  $-10^\circ\text{C}$  provides the cationic methallyl complexes,  $\text{Cp}^*\text{Zr}(\eta^3\text{-C}_4\text{H}_7)[\text{N}(\text{R}^1)\text{C}(\text{Me})\text{N}(\text{R}^2)]$  (**2a**:  $\text{R}^1 = \text{R}^2 = i\text{-Pr}$  and **2b**:  $\text{R}^1 = \text{Et}$ ,  $\text{R}^2 = t\text{-Bu}$ ), which are thermally robust in solution at elevated temperatures as determined by  $^1\text{H}$  NMR spectroscopy. Addition of  $\text{B}(\text{C}_6\text{F}_5)_3$  to **1a** and **1b** provides the zwitterionic allyl complexes,  $\text{Cp}^*\text{Zr}\{\eta^3\text{-CH}_2\text{C}[\text{CH}_2\text{B}(\text{C}_6\text{F}_5)_3]\text{CH}_2\}[\text{N}(\text{R}^1)\text{C}(\text{Me})\text{N}(\text{R}^2)]$  (**3a**:  $\text{R}^1 = \text{R}^2 = i\text{-Pr}$  and **3b**:  $\text{R}^1 = \text{Et}$ ,  $\text{R}^2 = t\text{-Bu}$ ). The crystal structures of **2b** and **3a** have been determined. Neither the cationic complexes **2** or the zwitterionic complexes **3** are active initiators for the Ziegler-Natta polymerization of ethylene and  $\alpha$ -olefins.

© 2003 Elsevier Science B.V. All rights reserved.

**Keywords:** Ziegler-Natta polymerization; Cationic allyl complexes; Zwitterionic allyl complexes

## 1. Introduction

Cationic zirconium allyl complexes have been implicated as playing critical roles in the deactivation of zirconocene-based propagating species involved in the Ziegler-Natta polymerization of  $\alpha$ -olefins [1], and possibly, in the formation of stereoerrors that occur during such polymerizations carried out at reduced monomer concentrations [2,3]. In a recent study, Brintzinger and co-workers [4] investigated the rate of propene insertion into the methallyl ligand of the cationic zirconocene complex,  $[(\eta^5\text{-C}_5\text{H}_5)_2\text{Zr}(\eta^3\text{-C}_4\text{H}_7)]^+[\text{MeB}(\text{C}_6\text{F}_5)_3]^-$ , which serves as a model for an allyl complex carrying a polymer alkyl chain, and found it to be significantly lower than rates of propene insertion into the zirconium-carbon bond of cationic zirconium alkyl species. On the other hand, Erker and co-workers [5] demonstrated that the zwitterionic zirconocene allyl-borate species,  $(\eta^5\text{-C}_5\text{H}_5)_2\text{Zr}[\eta^3\text{-CH}_2\text{CHCH}_2\text{-}$

$\text{B}(\text{C}_6\text{F}_5)_3]$ , derived from reaction of a zirconocene butadiene complex with  $\text{B}(\text{C}_6\text{F}_5)_3$ , can serve as a highly active initiator for the Ziegler-Natta polymerization of propene. Given the opposing behavior presented by these two cases, there is a clear need to further establish the structural and electronic factors that govern the barriers to olefin insertion into allyl ligands of cationic and zwitterionic zirconium complexes, and in particular, of non-metallocene-based Ziegler-Natta initiators and propagating species. With respect to this, we recently reported that cationic cyclopentadienylzirconium acetamidinates of the general structure,  $[(\eta^5\text{-C}_5\text{R}_5)\text{-ZrX}\{\text{N}(\text{R}^1)\text{C}(\text{Me})\text{N}(\text{R}^2)\}]^+[\text{B}(\text{C}_6\text{F}_5)_4]^-$ , are highly active initiators for the living Ziegler-Natta polymerization of  $\alpha$ -olefins and  $\alpha, \omega$ -nonconjugated dienes, and where  $\text{R} = \text{X} = \text{Me}$ ,  $\text{R}^1 = \text{Et}$  and  $\text{R}^2 = t\text{-Bu}$ , these polymerizations proceed in an isospecific fashion [6]. Further, in the pursuit of structurally related cationic zirconium alkyl derivatives that might prove useful as either initiators or models of the propagating species (e.g.,  $\text{X} = i\text{-Bu}$ ), it was discovered that the neutral diisobutyl cyclopentadienylzirconium acetamidinates,  $\text{Cp}^*\text{Zr}(i\text{-Bu})_2[\text{N}(\text{R}^1)\text{C}(\text{Me})\text{N}(\text{R}^2)]$  ( $\text{Cp}^* = \eta^5\text{-C}_5\text{Me}_5$ )

\* Corresponding author. Tel.: +1-301-405-5753; fax: +1-301-314-9121.

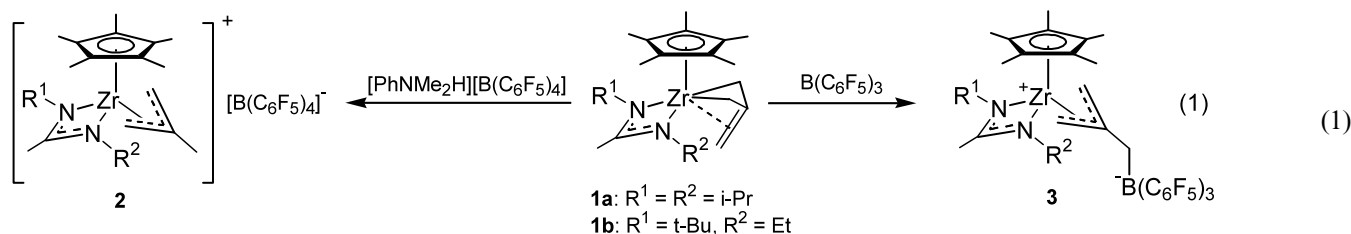
E-mail address: [ls214@umail.umd.edu](mailto:ls214@umail.umd.edu) (L.R. Sita).

( $R^1 = R^2 = i\text{-Pr}$  and  $R^1 = \text{Et}$ ,  $R^2 = t\text{-Bu}$ ), decomposed at 50 °C in solution to provide the novel  $\sigma^2, \pi$ -trimethylenemethane (TMM) cyclopentadienylzirconium acetamidinates,  $\text{Cp}^*\text{Zr}(\sigma^2, \pi\text{-C}_4\text{H}_6)[\text{N}(\text{R}^1)\text{C}(\text{Me})\text{N}(\text{R}^2)]$  (**1a** and **1b**, respectively), albeit not in highly reproducible amounts given the apparent complexity of the decomposition mechanism [7,8]. With these compounds in hand, however, we were immediately interested in determining whether they could be viable precursors to Ziegler-Natta cationic or zwitterionic allyl zirconium initiators or model complexes through direct ‘activation’ with either borate or borane reagents, respectively, according to Eq. (1). In the present work, we now present a reliable direct synthesis of the TMM compounds **1a** and **1b**, the results of more extensive solution and solid-state structural characterizations of these species, and a documentation of their utility as precursors to the cationic and zwitterionic allyl zirconium complexes, **2** and **3**, respectively, shown in Eq. (1).

method that involved the use of a two-fold excess of *n*-butyllithium [9].  $\text{B}(\text{C}_6\text{F}_5)_3$  and  $[\text{PhNMe}_2\text{H}][\text{B}(\text{C}_6\text{F}_5)_4]$  were obtained from Aldrich and Boulder Scientific, respectively, and used without further purification.  $^1\text{H}$  and  $^{13}\text{C}\{^1\text{H}\}$  NMR spectra were recorded at 400 (or 500) and 100 MHz, respectively, using either benzene- $d_6$ , toluene- $d_6$  (VT NMR experiments) or chlorobenzene- $d_5$  as the solvent. Elemental analyses were performed by Midwest Microlab.

## 2.2. Synthesis of $\text{Cp}^*\text{Zr}(\sigma^2, \pi\text{-C}_4\text{H}_6)[\text{N}(i\text{-Pr})\text{C}(\text{Me})\text{N}(i\text{-Pr})]$ (**1a**)

To a suspension of 0.63 g (2.30 mmol) of  $\text{K}_2(\text{TMM})$  in 70 ml of pentane, cooled to  $-78$  °C, a solution of 1.03 g (2.30 mmol) of **4a** in 5 ml of THF was added dropwise. The resulting mixture was allowed to warm up to ambient temperature during 2 h, whereupon, the volatiles were removed in vacuo. The residue was then



## 2. Experimental

### 2.1. General procedures

Manipulations were performed under an inert atmosphere of dinitrogen using standard Schlenk techniques or a Vacuum Atmospheres glovebox. Dry, oxygen-free solvents were employed throughout. Diethyl ether ( $\text{Et}_2\text{O}$ ), tetrahydrofuran (THF) and pentane were distilled from sodium/benzophenone (with a few milliliters of triglyme being added to the pot in the case of pentane), and chlorobenzene ( $\text{PhCl}$ ) was refluxed for several days over calcium hydride before being used for polymerizations. The monomer 1-hexene (99%) was obtained from Aldrich and stirred over NaK alloy (1:1) overnight before being vacuum-transferred. Benzene- $d_6$  was likewise vacuum transferred from NaK prior to being used for NMR spectroscopy. Chlorobenzene- $d_5$  was dried over CaH prior to vacuum transfer.  $\text{Cp}^*\text{ZrCl}_2[\text{N}(i\text{-Pr})\text{C}(\text{Me})\text{N}(i\text{-Pr})]$  and  $\text{Cp}^*\text{ZrCl}_2[\text{N}(\text{Et})\text{C}(\text{Me})\text{N}(t\text{-Bu})]$  (**4a** and **4b**, respectively) were prepared as previously reported [7] and  $\text{K}_2(\text{TMM})$  was prepared according to a slight modification of the literature

extracted with pentane, the extracts filtered through a small pad of Celite, and the solvent removed in vacuo to provide a crude material that was recrystallized at  $-30$  °C from a 5:1 pentane/toluene mixture (ca. 4 ml) to give 0.51 g (51% yield) of **1a** as a red crystalline material. For **1a**:  $^1\text{H}$  NMR (benzene- $d_6$ , 25 °C):  $\delta$  0.77, 0.80 (d, 6H,  $J = 6.4$  Hz,  $\text{CHMe}_2$ ); 1.52 (s, 3H,  $\text{CMe}$ ); 1.91 (s, 15H,  $\text{C}_5\text{Me}_5$ ); 2.57 (br s, 6H,  $\text{C}(\text{CH}_2)_3$ ); 3.38 (sept, 2H,  $J = 6.4$  Hz,  $\text{CHMe}_2$ ).  $^{13}\text{C}\{^1\text{H}\}$  NMR (benzene- $d_6$ , 25 °C):  $\delta$  12.1 ( $\text{C}_5\text{Me}_5$ ); 12.7 ( $\text{CMe}$ ); 24.8, 25.5 ( $\text{CHMe}_2$ ); 47.6 ( $\text{CHMe}_2$ ); 75.5 ( $\text{C}(\text{CH}_2)_3$ ); 119.5 ( $\text{C}_5\text{Me}_5$ ), 163.8, 165.4 ( $\text{CMe}$ ,  $\text{C}(\text{CH}_2)_3$ ). Anal. Calc. for  $\text{C}_{22}\text{H}_{38}\text{N}_2\text{Zr}$ : C, 62.65; H, 9.08; N, 6.64. Found: C, 61.86; H, 8.86; N, 6.05.

### 2.3. Synthesis of $\text{Cp}^*\text{Zr}(\sigma^2, \pi\text{-C}_4\text{H}_6)[\text{N}(t\text{-Bu})\text{C}(\text{Me})\text{N}(\text{Et})]$ (**1b**)

In the glovebox, 0.68 g (2.48 mmol) of solid  $\text{K}_2(\text{TMM})$  was added to a suspension of 1.09 g (2.49 mmol) of **4b** in 30 ml of a 10:1  $\text{Et}_2\text{O}$ /pentane mixture, cooled to ca.  $-30$  °C in an internal refrigerator. The resulting mixture was then allowed to gradually warm

up to ambient temperature. After stirring overnight, the volatiles were removed in vacuo, the residue was extracted with pentane, the extracts filtered through a small pad of Celite, and then the solvent removed in vacuo to provide a crude material that was recrystallized at  $-30\text{ }^{\circ}\text{C}$  from a 5:1 pentane/toluene mixture (ca. 6 ml) to provide 0.24 g (23% yield) of **1b** as a red crystalline material. For **1b**:  $^1\text{H}$  NMR (benzene- $d_6$ ,  $25\text{ }^{\circ}\text{C}$ ):  $\delta$  0.87 (t, 3H,  $J=7.2$  Hz,  $\text{CH}_2\text{CH}_3$ ); 0.92 (s, 9H,  $\text{CMe}_3$ ); 1.56 (s, 3H,  $\text{CMe}$ ); 1.87 (s, 15H,  $\text{C}_5\text{Me}_5$ ); 2.57 (br s, 6H,  $\text{C}(\text{CH}_2)_3$ ); 2.89 (dq, 1H,  $^2J=13.8$  Hz,  $^3J=7.2$  Hz,  $\text{CH}_A\text{H}_B\text{CH}_3$ ), 2.91 (dq, 1H,  $^2J=13.8$  Hz,  $^3J=7.2$  Hz,  $\text{CH}_A\text{H}_B\text{CH}_3$ ).  $^{13}\text{C}$   $\{^1\text{H}\}$  NMR (benzene- $d_6$ ,  $25\text{ }^{\circ}\text{C}$ ):  $\delta$  11.7 ( $\text{C}_5\text{Me}_5$ ); 14.4 ( $\text{CMe}$ ); 17.1 ( $\text{CH}_2\text{CH}_3$ ); 31.2 ( $\text{CMe}_3$ ); 41.5 ( $\text{CH}_A\text{H}_B\text{CH}_3$ ); 53.0 ( $\text{CMe}_3$ ), 74.4 ( $\text{C}(\text{CH}_2)_3$ ); 118.3 ( $\text{C}_5\text{Me}_5$ ), 165.0, 166.8 ( $\text{CMe}$ ,  $\text{C}(\text{CH}_2)_3$ ). Anal. Calc. for  $\text{C}_{22}\text{H}_{38}\text{N}_2\text{Zr}$ : C, 62.65; H, 9.08; N, 6.64. Found: C, 61.86; H, 8.86; N, 6.05.

#### 2.4. NMR investigation of protonation of $\text{Cp}^*\text{Zr}(\sigma^2, \pi\text{-C}_4\text{H}_6)[\text{N}(\text{R}^1)\text{C}(\text{Me})\text{N}(\text{R}^2)]$ (**1a**: $\text{R}^1 = \text{R}^2 = i\text{-Pr}$ ; **1b**: $\text{R}^1 = \text{Et}$ , $\text{R}^2 = t\text{-Bu}$ ) using $[\text{PhNMe}_2\text{H}][\text{B}(\text{C}_6\text{F}_5)_4]$

A solution of **1a** or **1b** (0.02 mmol in ca. 0.5 ml of chlorobenzene- $d_5$ ) was added to a suspension of 16 mg (0.02 mmol) of  $[\text{PhNMe}_2\text{H}][\text{B}(\text{C}_6\text{F}_5)_4]$  in ca. 0.3 ml of chlorobenzene- $d_5$  at ambient temperature. The resulting clear red–orange solution of the cationic species **2a** or **2b** was then transferred to a NMR tube. In the case of **2b**, upon cooling to  $-20\text{ }^{\circ}\text{C}$ , small orange–red crystals deposited upon the walls of the NMR after several weeks. Although insufficient material was obtained for chemical analysis, these crystals proved suitable for single crystal X-ray analysis.

##### 2.4.1. For compound **2a**

$^1\text{H}$  NMR (chlorobenzene- $d_5$ ,  $25\text{ }^{\circ}\text{C}$ ):  $\delta$  0.92 (d, 6H,  $J=6.4$  Hz,  $\text{CHMe}_2$ ), 1.03 (d, 6H,  $J=6.4$  Hz,  $\text{CHMe}_2$ ); 2.05 (s, 3H,  $\text{CMe}$ ); 2.07 (s, 18H,  $\text{C}_5\text{Me}_5$ ,  $\text{CH}_2\text{C}(\text{Me})\text{CH}_2$ ); 3.0 (s, 2H,  $\text{CH}_2\text{C}(\text{Me})\text{CH}_2$ ), 3.18 (s, 2H,  $\text{CH}_2\text{C}(\text{Me})\text{CH}_2$ ); 3.51 (sept, 2H,  $J=6.4$  Hz,  $\text{CHMe}_2$ ).

##### 2.4.2. For compound **2b**

$^1\text{H}$  NMR (chlorobenzene- $d_5$ ,  $25\text{ }^{\circ}\text{C}$ ):  $\delta$  0.82, (t, 3H,  $J=7.0$  Hz,  $\text{CH}_2\text{CH}_3$ ); 0.92 (s, 9H,  $\text{CMe}_3$ ); 1.85 and 1.90 (s, 21H,  $\text{C}_5\text{Me}_5$ ,  $\text{CH}_2\text{C}(\text{Me})\text{CH}_2$ ,  $\text{CMe}$ ); 2.73 (br s, 1H,  $\text{CH}_2\text{C}(\text{Me})\text{CH}_2$ ), 2.97 (br s, 1H,  $\text{CH}_2\text{C}(\text{Me})\text{CH}_2$ ), 3.04 (br s, 1H,  $\text{CH}_2\text{C}(\text{Me})\text{CH}_2$ ); 2.88 (m, 2H,  $\text{CH}_A\text{H}_B\text{CH}_3$ ). Note: the resonance for  $\text{PhNMe}_2$  is presumed to be obscuring a methallyl resonance at 2.68 ppm.

#### 2.5. Synthesis of $\text{Cp}^*\text{Zr}\{\eta^3\text{-CH}_2\text{C}[\text{CH}_2\text{B}(\text{C}_6\text{F}_5)_3]\text{CH}_2\}\{\text{N}(i\text{-Pr})\text{C}(\text{Me})\text{N}(i\text{-Pr})\}$ (**3a**)

Within a glovebox, a solution of 182 mg (0.43 mmol) of **1a** in 1 ml of chlorobenzene was added to a solution of 100 mg (0.43 mmol) of  $\text{B}(\text{C}_6\text{F}_5)_3$  in 1 ml of chlorobenzene at ambient temperature. The solution was then layered with pentane (ca. 10 ml) and stored overnight at  $-30\text{ }^{\circ}\text{C}$  in an internal refrigerator to give red–orange crystals of **3a** (228 mg, 82% yield). For compound **3a**:  $^1\text{H}$  NMR (chlorobenzene- $d_5$ ,  $25\text{ }^{\circ}\text{C}$ ):  $\delta$  0.67 (d, 6H,  $J=6.0$  Hz,  $\text{CHMe}_2$ ), 0.71 (d, 6H,  $J=6.0$  Hz,  $\text{CHMe}_2$ ); 1.70 (s, 15H,  $\text{C}_5\text{Me}_5$ ); 1.93 (s, 3H,  $\text{CMe}$ ); 2.57 (s, 2H,  $\text{CH}_2\text{C}[\text{CH}_2\text{B}(\text{C}_6\text{F}_5)_3]\text{CH}_2$ ), 2.71 (s, 2H,  $\text{CH}_2\text{C}[\text{CH}_2\text{B}(\text{C}_6\text{F}_5)_3]\text{CH}_2$ ); 2.57 (br s, 2H,  $\text{CH}_2\text{C}[\text{CH}_2\text{B}(\text{C}_6\text{F}_5)_3]\text{CH}_2$ ); 3.38 (sept, 2H,  $J=6.0$  Hz,  $\text{CHMe}_2$ ).  $^{13}\text{C}$   $\{^1\text{H}\}$  NMR (chlorobenzene- $d_5$ ,  $25\text{ }^{\circ}\text{C}$ ):  $\delta$  10.9, 12.0, 21.0, 22.4, 40.6, 48.9, 88.1, 124.5, 173.3, 189.9, Anal. Calc. for  $\text{C}_{40}\text{H}_{38}\text{BF}_{15}\text{N}_2\text{Zr}$ : C, 51.45; H, 4.10; N, 3.0. Found: C, 51.21; H, 4.18; N, 3.04.

#### 2.6. Crystal structure determinations

Data were collected on a Bruker SMART CCD system operating at  $-80\text{ }^{\circ}\text{C}$ . All crystallographic calculations were performed on a personal computer with a Pentium 1.80 GHz processor and 512 MB of extended memory. The SHELXTL program package was implemented to determine the probable space group and set up the initial files. Table 1 provides information on the data collection and refinement parameters for compounds **2b** and **3a**.

#### 2.7. Crystal structure determination of compound **2b**

An orange block with approximate orthogonal dimensions  $0.23 \times 0.21 \times 0.17\text{ mm}^3$  was placed and optically centered on the Bruker SMART CCD system at  $-100\text{ }^{\circ}\text{C}$ . The initial unit cell was indexed using a least-squares analysis of a random set of reflections collected from three series of  $0.3^{\circ}$  wide  $\omega$ -scans, 10 s per frame, and 25 frames per series that were well distributed in reciprocal space. Data frames were collected  $[\text{Mo-K}\alpha]$  with  $0.2^{\circ}$  wide  $\omega$ -scans, 40 s per frame and 909 frames per series. Six data series were collected, five at varying  $\varphi$  angles ( $\varphi=0^{\circ}$ ,  $72^{\circ}$ ,  $144^{\circ}$ ,  $216^{\circ}$ ,  $288^{\circ}$ ), a sixth composed of 909  $0.2^{\circ}$  wide  $\varphi$ -scans with fixed  $\omega=-30^{\circ}$  and finally a partial repeat of the first series, 200 frames, for decay purposes. The crystal to detector distance was 4.442 cm, thus providing a complete sphere of data to  $2\theta_{\text{max}}=55.1^{\circ}$ . A total of 86458 reflections were collected and corrected for Lorentz and polarization effects and absorption using Blessing's method as incorporated into the program SADABS with 10738 unique [ $R_{\text{int}}=0.0379$ ]. System symmetry, systematic

Table 1  
Crystallographic data and details of refinement for compounds **2b** and **3a**

	<b>2b</b>	<b>3b</b>	
		<i>C2/c</i>	<i>P</i> $\bar{1}$
Empirical formula	C <sub>46</sub> H <sub>39</sub> BF <sub>20</sub> N <sub>2</sub> Zr	[C <sub>40</sub> H <sub>38</sub> BF <sub>15</sub> N <sub>2</sub> Zr][C <sub>6</sub> H <sub>5</sub> Cl] <sub>1.5</sub>	[C <sub>40</sub> H <sub>38</sub> BF <sub>15</sub> N <sub>2</sub> Zr][C <sub>6</sub> H <sub>5</sub> Cl]
Formula weight	1101.82	1102.58	1046.30
Temperature (K)	173(2)	173(2)	173(2)
Crystal system	monoclinic	monoclinic	triclinic
Space group	<i>P2</i> <sub>1</sub> / <i>n</i>	<i>C2/c</i>	<i>P</i> $\bar{1}$
<i>a</i> (Å)	13.1664(6)	22.320(4)	10.5876(3)
<i>b</i> (Å)	23.2144(11)	10.7833(18)	12.2659(4)
<i>c</i> (Å)	15.2561(7)	39.856(7)	18.1468(5)
$\alpha$ (°)	90	90	95.4760(10)
$\beta$ (°)	103.6160(10)	98.711(3)	92.4220(10)
$\gamma$ (°)	90	90	107.8310(10)
<i>V</i> (Å <sup>3</sup> )	4532.0(4)	9482(3)	2226.85(11)
<i>Z</i>	4	8	2
$\rho_{\text{calc}}$ (g cm <sup>-3</sup> )	1.615	1.545	1.560
$\mu$ (Mo) (mm <sup>-1</sup> )	0.362	0.413	0.406
Crystal size (mm)	0.23 × 0.21 × 0.17	0.24 × 0.20 × 0.10	0.36 × 0.19 × 0.13
2 $\theta$ range (°)	1.82–25.00	1.85–25.00	2.19–30.00
Total reflections	31 283	63 505	51 284
Independent reflections	7980 [ <i>R</i> <sub>int</sub> = 0.0383]	8362 [ <i>R</i> <sub>int</sub> = 0.0416]	12 837 [ <i>R</i> <sub>int</sub> = 0.0253]
Data/restraints/parameters	7980/3/690	8362/6/817	12 837/7/742
Final <i>R</i> indices [ <i>I</i> > 2 $\sigma$ ( <i>I</i> )]	<i>R</i> <sub>1</sub> = 0.0448, <i>wR</i> <sub>2</sub> = 0.1226	<i>R</i> <sub>1</sub> = 0.0584, <i>wR</i> <sub>2</sub> = 0.1145	<i>R</i> <sub>1</sub> = 0.0378, <i>wR</i> <sub>2</sub> = 0.1076
<i>R</i> indices (all data)	<i>R</i> <sub>1</sub> = 0.0651, <i>wR</i> <sub>2</sub> = 0.1335	<i>R</i> <sub>1</sub> = 0.0666, <i>wR</i> <sub>2</sub> = 0.1165	<i>R</i> <sub>1</sub> = 0.0474, <i>wR</i> <sub>2</sub> = 0.1139
Goodness-of-fit	1.086	1.317	1.104

absences and intensity statistics indicated the centrosymmetric monoclinic non-standard space group *P2*<sub>1</sub>/*n* (no. 14). The structure was determined by direct methods with the successful location of nearly the entire molecule using the program *xs*<sup>4</sup>. The structure was refined with *XL*<sup>5</sup>. The 86 458 data collected were merged based upon identical indices yielding 41 531 data [*R*<sub>int</sub> = 0.0407] that were further truncated to 2 $\theta_{\text{max}}$  = 50.0° and merged and during least-squares refinement to 7980 unique data [*R*<sub>int</sub> = 0.00383]. A series of least-squares difference-Fourier cycles were required to locate the remaining non-hydrogen atoms. All full-occupancy non-hydrogen atoms were refined anisotropically. All of the hydrogen atoms were located directly from an additional difference-Fourier map and allowed to refine freely. Disorder was modeled for the ethyl and *t*-butyl groups. A centroid was calculated for the pentamethylcyclopentadienyl ligand. The final structure was refined to convergence [ $\Delta/\sigma \leq 0.001$ ] with *R*(*F*) = 6.51%, *wR*(*F*<sup>2</sup>) = 13.35%, GOF = 1.086 for all 7980 unique reflections [*R*(*F*) = 4.48%, *wR*(*F*<sup>2</sup>) = 12.26% for those 6174 data with *F*<sub>o</sub> > 4 $\sigma$ (*F*<sub>o</sub>)]. The final difference-Fourier map was featureless indicating that the structure is both correct and complete.

### 2.8. Crystal structure determination of compound **3a**

A reddish orange block with approximate orthogonal dimensions 0.24 × 0.2 × 0.10 mm<sup>3</sup> was placed and

optically centered on the Bruker SMART CCD system at –100 °C. The initial unit cell was indexed using a least-squares analysis of a random set of reflections collected from three series of 0.3° wide  $\omega$ -scans, 10 s per frame, and 25 frames per series that were well distributed in reciprocal space. Data frames were collected [Mo–K $\alpha$ ] with 0.3° wide  $\omega$ -scans, 40 s per frame and 606 frames per series. Five data series were collected at varying  $\phi$  angles [ $\phi = 0^\circ, 72^\circ, 144^\circ, 216^\circ, 288^\circ$ ], including a partial repeat of the first series, 200 frames, for decay purposes. The crystal to detector distance was 4.371 cm, thus providing a complete sphere of data to 2 $\theta_{\text{max}}$  = 50.0°. A total of 63 505 reflections were collected and corrected for Lorentz and polarization effects and absorption using Blessing's method as incorporated into the program *SADABS* with 8362 unique [*R*<sub>int</sub> = 0.0416]. System symmetry, systematic absences and intensity statistics indicated the centrosymmetric monoclinic non-standard space group *C2/c* (no. 15). The structure was determined by direct methods with the successful location of nearly the entire molecule of interest using the program *xs*. The structure was refined with *XL*. A single least-squares difference-Fourier cycle was required to locate the remaining non-hydrogen atoms. All non-hydrogen atoms were refined anisotropically. All of the hydrogen atoms were located directly from an additional difference-Fourier map and allowed to refine freely. A centroid was calculated for the pentamethylcyclopentadienyl ligand and also for the

allylic. The final structure was refined to convergence [ $\Delta/\sigma \leq 0.001$ ] with  $R(F) = 6.66\%$ ,  $wR(F^2) = 11.65\%$ ,  $GOF = 1.317$  for all 8362 unique reflections [ $R(F) = 5.84\%$ ,  $wR(F^2) = 11.45\%$  for those 7364 data with  $F_o > 4\sigma(F_o)$ ]. The final difference-Fourier map was featureless indicating that the structure is both correct and complete.

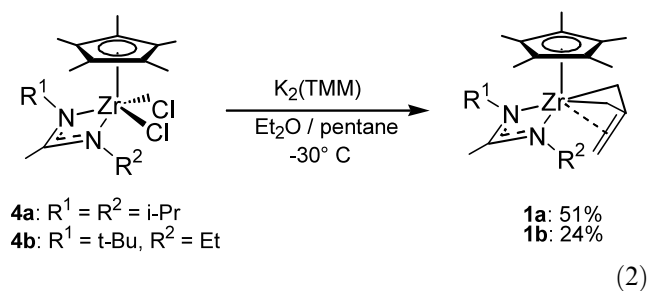
A second reddish orange block with approximate orthogonal dimensions  $0.362 \times 0.194 \times 0.125 \text{ mm}^3$  was placed and optically centered on the Bruker SMART CCD system at  $-100^\circ\text{C}$ . The initial unit cell was indexed using a least-squares analysis of a random set of reflections collected from three series of  $0.3^\circ$  wide  $\omega$ -scans, 10 s per frame, and 30 frames per series that were well distributed in reciprocal space. Data frames were collected [ $\text{Mo-K}\alpha$ ] with  $0.2^\circ$  wide  $\omega$ -scans, 20 s per frame and 909 frames per series. Six data series were collected, five at varying  $\varphi$  angles ( $\varphi = 0^\circ, 72^\circ, 144^\circ, 216^\circ, 288^\circ$ ), a sixth composed of 1200  $0.2^\circ$  wide  $\omega$ -scans with fixed  $\varphi = 0^\circ$  and finally, 200 frames, a partial repeat of the first series for decay purposes. The crystal to detector distance was 4.371 cm, thus providing a complete sphere of data to  $2\theta_{\text{max}} = 60.0^\circ$ . A total of 51 284 reflections were collected and corrected for Lorentz and polarization effects and absorption using Blessing's method as incorporated into the program SADABS with 12 837 unique [ $R_{\text{int}} = 0.0253$ ]. System symmetry, lack of systematic absences and intensity statistics indicated the centrosymmetric triclinic space group  $P\bar{1}$  (no. 2). The structure was determined by direct methods with the successful location of nearly the entire molecule of interest using the program xs. The structure was refined with XL. A series of least-squares difference-Fourier cycles were required to locate the remaining non-hydrogen atoms. All non-hydrogen atoms were refined anisotropically. All of the hydrogen atoms were located directly from an additional difference-Fourier map and allowed to refine freely. A centroid was calculated for the pentamethylcyclopentadienyl ligand and also for the allylic region of the large multidentate ligand. The final structure was refined to convergence [ $\Delta/\sigma \leq 0.001$ ] with  $R(F) = 4.74\%$ ,  $wR(F^2) = 11.39\%$ ,  $GOF = 1.104$  for all 12 837 unique reflections [ $R(F) = 3.78\%$ ,  $wR(F^2) = 10.76\%$  for those 10 968 data with  $F_o > 4\sigma(F_o)$ ]. The final difference-Fourier map was featureless indicating that the structure is both correct and complete.

### 3. Results and discussion

#### 3.1. Preparation of TMM complexes **1a** and **1b**

Although compounds **1a** and **1b** have previously been reported by us [7], reliable amounts of these TMM complexes were difficult to obtain due to the complexity

of the decomposition pathway leading to their formation that also produces difficult to separate crystalline coproducts [8]. Accordingly, a direct synthetic route to these materials was sought and as Eq. (2) reveals, this was secured through reaction of the corresponding dichloro cyclopentadienylzirconium acetamidates **4** [7] with the dipotassium salt of the trimethylenemethane dianion,  $\text{K}_2(\text{TMM})$  [9]. While the unoptimized yields of **1a** and **1b** that can be obtained by this procedure are modest for **1a** and low for **1b**, 51 and 24%, respectively, the amounts that can be obtained are reproducible and purification of the compounds can be achieved by a simple single recrystallization.



#### 3.2. Solid-state and solution structural studies of complexes **1a** and **1b**

Only three TMM derivatives of early transition metals other than **1a** and **1b** are known [10], and of these, only two have been the subject of crystallographic studies; anionic  $[\text{Cp}^*\text{Zr}(\text{TMM})\text{Cl}_2]^-$  (**5**) in which the TMM ligand is proposed to coordinate in a  $\eta^4$ -fashion [10b], and the neutral zirconocene,  $\text{Cp}^*\text{Zr}(\text{TMM})$  (**6**), in which the  $\eta^2$ -TMM group is clearly interacting with the metal center through only two  $\sigma$ -bonds. The  $\eta^2$ -TMM interaction of **6** will henceforth then be regarded as an example of  $\sigma^2$ -TMM bonding. To probe the nature of bonding in **1**, the crystal structures of **1a** and **1b** were obtained and presented in our initial report where we stated, without extensive comment, that their structural parameters supported a  $\sigma^2, \pi$ -TMM bonding mode [7]. Here, we now make a stronger case for this designation through a comparison of the molecular structures and selected structural parameters of **1a** and **1b** that are presented in Fig. 1 and Table 2, respectively. To begin, upon first inspection, compounds **1a** and **1b** would appear to present nearly identical structures with respect to the cyclopentadienyl, acetamidate, and TMM fragments. However, closer analysis reveals that, due most likely to increased steric interactions, the TMM moiety dissymmetrically lies closer to the N-Et side of the acetamidate in **1b** rather than being almost symmetrically disposed as in the structure of **1a** (cf. the nonbonded distances for N(1)–C(20) and N(2)–

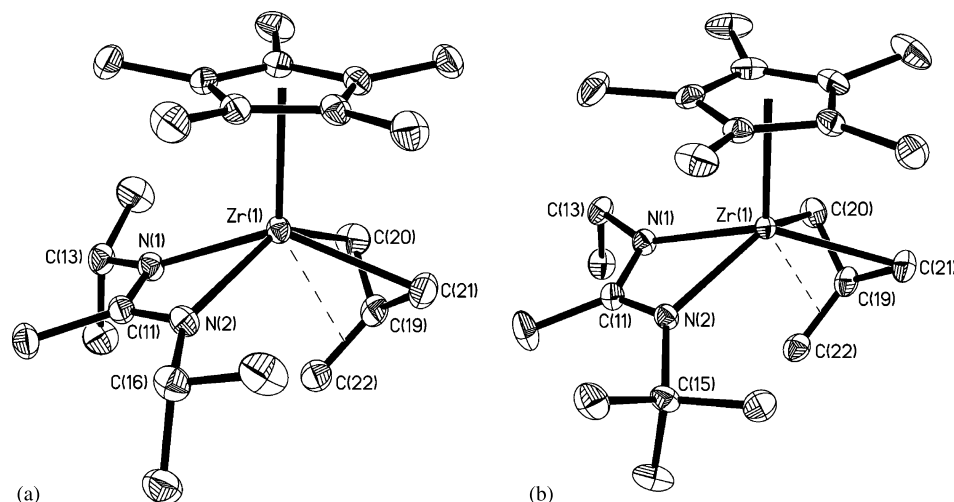


Fig. 1. Molecular structures (30% thermal ellipsoids) of (a) compound **1a** and (b) compound **1b**. Hydrogen atoms have been removed for the sake of clarity.

Table 2  
Selected distances (Å) and angles (°) for compounds **1a** and **1b**

	<b>1a</b>	<b>1b</b>
<i>Distances</i>		
Zr(1)–N(1)	2.2306(12)	2.2412(15)
Zr(1)–N(2)	2.2306(12)	2.2421(14)
Zr(1)–C(19)	2.3239(14)	2.3102(17)
Zr(1)–C(20)	2.3774(17)	2.4144(19)
Zr(1)–C(21)	2.3888(17)	2.3926(19)
C(19)–C(20)	1.442(2)	1.431(3)
C(19)–C(21)	1.440(3)	1.437(3)
C(19)–C(22)	1.385(2)	1.394(3)
Zr(1)–C(22)	2.642	2.553
N(1)–C(20)	3.462	3.149
N(2)–C(21)	3.763	4.103
<i>Angles</i>		
Zr(1)–N(1)–C(13)	145.7(10)	142.05(12)
Zr(1)–N(2)–C(16)	142.65(10)	–
Zr(1)–N(2)–C(15)	–	135.29(11)
C(20)–C(19)–C(21)	113.83(16)	113.77(19)
C(20)–C(19)–C(22)	116.86(18)	118.12(19)
C(21)–C(19)–C(22)	117.96(17)	116.2(2)

C(21) of 3.462 and 3.763 Å in **1a** vs. the corresponding distances of 3.149 and 4.103 Å in **1b**). The increased steric interactions in **1b** are also manifested in the slight pyramidalization observed for N(2) which bears the *tert*-butyl substituent (cf. the sum of the bond angles about N(2),  $\Sigma_{\theta}N(2) = 356.2^{\circ}$ , in **1b** vs.  $360^{\circ}$  for all the other nitrogen atoms in **1a** and **1b**). Regarding bonding to the TMM fragment, in both structures, the shortest zirconium–carbon distance is found between the metal and the central carbon atom, C(19), of the TMM group at 2.3239(14) Å in **1a** and 2.3102(17) Å in **1b**. In comparison, the zirconium–carbon distances involving C(20) and C(21) are significantly longer [cf. 2.3774(17); 2.3888(17) in **1a** and 2.4144(19); 2.3926(19) in **1b**], while

that involving C(22) now falls outside a conventional zirconium–carbon bonding distance [cf. 2.642 and 2.553 Å for **1a** and **1b**, respectively]. Within the TMM fragment itself, the C(19)–C(20) and C(19)–C(21) bond distances are distinctly longer in both complexes at 1.440(3); 1.442(2) in **1a** and 1.431(3); 1.437(3) in **1b** relative to that for the C(19)–C(22) bond for which the observed values are 1.385(2) for **1a** and 1.394(3) for **1b**. This last structural comparison suggests that the C(19)–C(22) bond has a greater degree of ‘double bond’ character which suggests that the  $\sigma^2, \pi$ -TMM bonding mode that is depicted in Fig. 1 is operative in both structures. It must be pointed out, however, that C(19) in both **1a** and **1b** is pyramidalized to a large extent as indicated by the bond angle sums for  $\Sigma_{\theta}C(19)$  of  $348.7^{\circ}$  in **1a** and  $348.0^{\circ}$  in **1b**. Thus, an argument could also be made for a strong contribution to Zr–TMM bonding of a  $\eta^4$ -interaction where the Zr(1)–C(22) bond is substantially elongated due to a strong *trans*-effect of the cyclopentadienyl group as originally proposed by Bazan et al. [10b]. To illuminate the TMM-bonding picture in **1** further, solution studies involving variable temperature  $^1\text{H}$  NMR spectroscopy of **1a** and **1b** were carried out.

At room temperature,  $^1\text{H}$  NMR spectra showed that the TMM fragments in **1a** and **1b** are not static on the NMR timeframe, but rather, they are engaged in a dynamic process that serves to exchange certain sets of formally magnetically inequivalent protons by ‘rotation’ of the TMM group about the Zr(1)–C(19) ‘bond’. Due to the  $C_s$ -symmetric nature of **1a**, all six protons of the TMM group are expected to become equivalent from this process, whereas the  $C_1$ -symmetry of **1b** should compartmentalize the six protons into two sets of three site-exchanging protons, if a TMM ‘face-flipping’ process does not additionally exist. For **1a**, an apparent slow exchange limit  $^1\text{H}$  NMR (400 MHz, toluene- $d_8$ ) spectrum taken at  $-80^{\circ}\text{C}$  revealed three separate

resonances at 1.56 (2H), 2.19 (2H) and 4.32 (2H) ppm for three sets of magnetically inequivalent protons expected for a static TMM group. The higher field resonances at 1.56 and 2.19 ppm are assigned to being those for the diastereotopic protons on the carbon atoms that are  $\sigma$ -bonded to zirconium within the  $\sigma^2, \pi$ -bonding scheme (i.e. C(20) and C(21) in Fig. 1). The remaining downfield resonance at 4.32 ppm is then assigned to belonging to the magnetically equivalent protons on the carbon which is postulated as having significant  $sp^2$ -character due to its involvement in the formal double bond within this same  $\sigma^2, \pi$ -bonding scheme (i.e. C(22) in Fig. 1). The absence of coupling between the two sets of diastereomeric protons indicated, however, that dynamic exchange was still occurring at an appreciable rate even at  $-80^\circ\text{C}$  and this assumption was verified by a 2D  $^1\text{H}$  EXSY spectrum taken at this temperature which produced significant crosspeaks for the exchanging protons within a wide range of mixing times [11]. Upon warming, coalescence of all three resonances for the TMM group was observed to occur at  $-40^\circ\text{C}$  and at  $25^\circ\text{C}$ , a broad singlet for these six protons materialized at 2.53 ppm. A similarly low barrier for TMM group rotation was

obtained previously for  $\text{Cp}^*\text{Ta}(\text{TMM})\text{Me}_2$  [10a], but in sharp contrast, a high barrier for this process was reported for the Zr-TMM complex **5**, and compound **6** apparently does not engage in TMM rotation at all [10b,10c].

Fig. 2 shows selected variable temperature  $^1\text{H}$  NMR spectra for **1b** taken at the apparent slow exchange limit, at coalescence, and above the coalescence temperature of the dynamic process involving TMM group rotation. In keeping with expectations, the apparent slow exchange limit  $^1\text{H}$  NMR spectrum for **1b** displays the expected six resonances for each of the six magnetically inequivalent protons of the TMM group within the static structure ( $\delta$  1.48, 1.96, 2.07, 2.50, 3.74, and 4.21 ppm). Qualitatively, the barrier to rotation in this complex is higher than that of **1a** presumably as a result of the increased steric interactions of the TMM and acetamidinate fragments discussed earlier. Importantly, the fast exchange spectrum taken at  $70^\circ\text{C}$  reveals two sets of resonances for the TMM fragment at 2.37 and 2.50 ppm (3H each) which demonstrates that neither face-flipping of the TMM, or any change in its hapticity that would serve to exchange any two diastereomeric protons, occurs at these elevated temperatures.

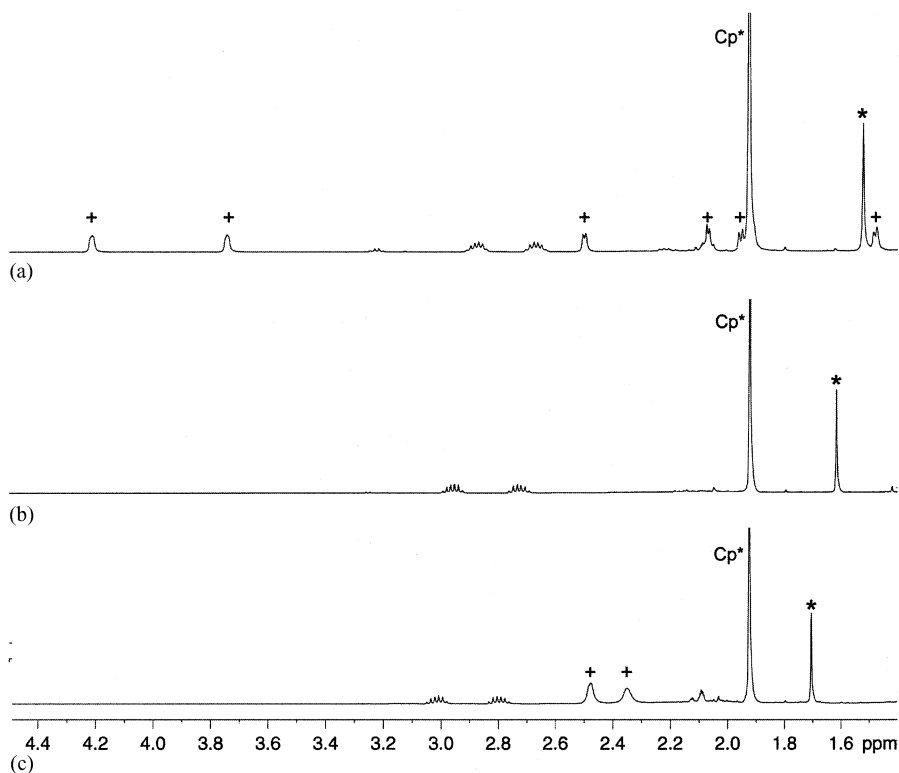


Fig. 2. Partial  $^1\text{H}$  NMR (400 MHz, toluene- $d_8$ ) spectra of **1b** recorded at (a)  $-70^\circ\text{C}$ , (b) the coalescence temperature of  $-10^\circ\text{C}$ , and (c)  $60^\circ\text{C}$ . The resonance for the methyl substituent of the acetamidinate group is marked with an asterisk (\*) and the resonances for the TMM fragment are indicated by pluses (+). The two resonances appearing in the range of 2.7–3.1 ppm are for the two diastereotopic protons of the N-Et substituent of the acetamidinate group.

### 3.3. Generation of cationic methallyl complexes **2a** and **2b** and the solid-state structure of **2b**

Attempts by Brintzinger and co-workers [4] to generate the cationic zirconocene complex,  $[(\eta^5\text{-C}_5\text{H}_5)_2\text{Zr}(\eta^3\text{-C}_4\text{H}_7)]^+$ , possessing the less strongly bound borate anion,  $[\text{B}(\text{C}_6\text{F}_5)_4]^-$ , were thwarted by non selective protonation of both the methyl and methallyl groups of  $(\eta^5\text{-C}_5\text{H}_5)_2\text{ZrMe}(\eta^3\text{-C}_4\text{H}_7)$  by  $[\text{PhNMe}_2\text{H}][\text{B}(\text{C}_6\text{F}_5)_4]$ . Indeed, to the best of our knowledge, such ‘looser’ ion pairs of cationic zirconium allyl complexes have yet to be prepared and characterized. Accordingly, it was with great satisfaction that it was found that addition of 1 equivalent of  $[\text{PhNMe}_2\text{H}][\text{B}(\text{C}_6\text{F}_5)_4]$  to either **1a** or **1b** in chlorobenzene at 25 °C resulted in quantitative formation of the cationic methallyl complexes, **2a** and **2b**, as determined by  $^1\text{H}$  NMR spectroscopy (see Eq. (1)). More specifically, an apparent static NMR spectrum was obtained for **2a** at 20 °C in chlorobenzene- $d_5$  that shows two sharp methylene resonances for the methallyl ligand at 2.85 and 3.02 ppm and two resonances for the diastereotopic methyl groups of the isopropyl substituents on the acetamidinate fragment at 0.75 and 0.86 ppm. Warming the NMR sample of **2a** eventually led to coalescence of the two methylene resonances at 60 °C for which a  $\eta^3 \rightarrow \eta^1$  allyl rearrangement barrier of  $\Delta G_{\ddagger}^{\ddagger} = 16.2 \text{ kcal mol}^{-1}$  could be estimated. This barrier is slightly higher than that observed for the similar process in  $[(\eta^5\text{-C}_5\text{H}_5)_2\text{Zr}(\eta^3\text{-C}_4\text{H}_7)]^+[\text{MeB}(\text{C}_6\text{F}_5)_4]^-$  [4] and it can most likely be attributed to the somewhat stronger preference for  $\eta^3$ -coordination of the methallyl ligand in **2a** due to an increased charge separation in the ion pair. The room temperature  $^1\text{H}$  NMR spectrum for

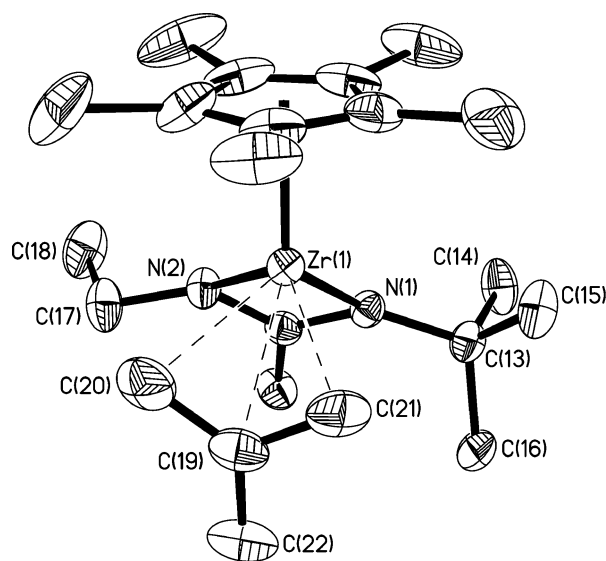


Fig. 3. Molecular structure (30% thermal ellipsoids) of compound **2b**. Hydrogen atoms and the  $[\text{B}(\text{C}_6\text{F}_5)_4]$  counterion have been removed for the sake of clarity.

Table 3  
Selected bond distances (Å) and angles (°) for compounds **2b** and **3a**

	<b>2b</b>	<b>3a</b>	
		C2/c	Pī
<i>Distances</i>			
Zr(1)–N(1)	2.149(3)	2.190(4)	2.2022(14)
Zr(1)–N(2)	2.188(3)	2.162(4)	2.1586(14)
Zr(1)–C(19)	2.500(4)	2.512(4)	2.4991(15)
Zr(1)–C(20)	2.448(5)	2.392(4)	2.3864(16)
Zr(1)–C(21)	2.395(4)	2.432(5)	2.4714(17)
B(1)–C(22)	–	1.684(6)	1.687(2)
C(19)–C(20)	1.374(7)	1.411(6)	1.413(2)
C(19)–C(21)	1.378(6)	1.398(6)	1.406(3)
C(19)–C(22)	1.500(6)	1.477(6)	1.493(2)
<i>Angles</i>			
Zr(1)–N(1)–C(13)	136.1(2)	144.6(3)	144.90(14)
Zr(1)–N(2)–C(16)	–	145.5(3)	143.74(12)
Zr(1)–N(2)–C(17)	138.7(2)	–	–
C(20)–C(19)–C(21)	119.0(5)	117.5(4)	117.16(16)
C(20)–C(19)–C(22)	120.8(5)	229.6(4)	120.29(15)
C(21)–C(19)–C(22)	118.4(5)	121.2(4)	120.50(16)
C(19)–C(22)–B(1)	–	114.1(3)	113.07(13)

**2b** recorded in chlorobenzene- $d_5$  similarly showed an apparent static structure. Finally, it can be mentioned that both **2a** and **2b** are quite robust in solution at elevated temperatures with no indication of decomposition after several hours according to  $^1\text{H}$  NMR.

Upon cooling the NMR sample of **2b** to  $-10$  °C, a small number of orange–red crystals were deposited upon the walls of the NMR tube after several weeks. Single crystal X-ray analysis confirmed that these crystals were that of **2b** and Fig. 3 and Table 3 respectively present the molecular structure and selected structural parameters for this complex. Of particular note are the zirconium–nitrogen bond distances of 2.149(3) and 2.188(3) Å in **2b** which are significantly shorter than those found for the neutral TMM complexes **1a** and **1b**. The methallyl fragment comprising C(19), C(20), C(21), and C(22) possesses geometrical parameters that are consistent with  $\eta^3$ -allyl ligation where the shortest zirconium–carbon contacts are found for the Zr(1)–C(20) and Zr(1)–C(21) distances. It must also be noted that no close contacts between the electrophilic zirconium center and any fluorine atoms of the borate counterion (not shown for the sake the clarity) are observed in the solid state packing scheme.

### 3.4. Preparation and characterization of the zwitterionic complexes **3a** and **3b**

Following the example of Erker and co-workers [5], we were interested in determining whether addition of  $\text{B}(\text{C}_6\text{F}_5)_3$  to **1a** and **1b** would provide the corresponding zwitterionic allyl–borate complexes **3a** and **3b** according to Eq. (1). Satisfactorily, addition of 1 equivalent of this

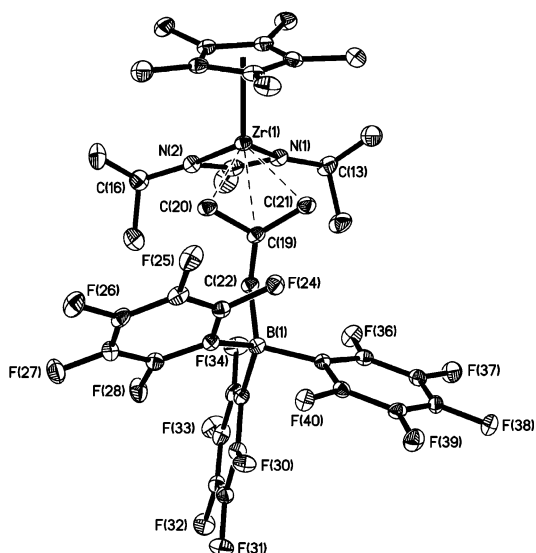


Fig. 4. Molecular structure (30% thermal ellipsoids) of compound **3a** from the monoclinic  $C2/c$  crystalline form. Hydrogen atoms have been removed for the sake of clarity.

borane to the TMM complexes **1** in chlorobenzene at room temperature led to instantaneous formation of a red–orange colored solution, from which, red crystals could be obtained in the case of **3a** upon addition of pentane and cooling to  $-10\text{ }^\circ\text{C}$ . Single-crystal X-ray analysis revealed the existence of two different crystalline polymorphs,  $C2/c$  and  $P\bar{1}$  modifications, that possess different solid-state structures for **3a**. As Figs. 4 and 5 and Table 3 show, the differences in these two structures mainly involve the relative orientation of the two isopropyl substituents on the acetamidinate fragments. In the  $P\bar{1}$  modification, it would appear from Fig. 5 that the isopropyl groups might be engaged in stronger steric interactions with the allyl fragment than in the  $C2/c$  polymorph. However, an inspection of the

structural parameters suggest that no significant differences between the two structures exist apart from the observation that the nitrogen atoms are slightly more pyramidalized in the  $P\bar{1}$  structure vs. those of the  $C2/c$  modification. This observation is consistent with our previous experiences where it has been noted that the soft potential surface for the amidinate group allows it to accommodate otherwise strong steric interactions within a structure through distortions that incur little or no energy penalties. Comparing the structure of **3a** to those of **1a** and **1b**, it is interesting to note that the carbon atoms of the allyl moiety in the former [i.e. C(19), C(20), and C(21)] are all positioned further away from the zirconium center than the corresponding atoms within the TMM derivatives. Finally, it can be noted that C(19) in **3a** is essentially trigonal coplanar with a  $\Sigma_\theta C(19)$  value of  $358^\circ$  in both crystalline modifications.

With respect to solution studies of **3a** and **3b**, variable temperature  $^1\text{H}$  NMR spectra revealed a static  $\eta^3$ -allyl structure for these compounds in the temperature range of  $20\text{--}120\text{ }^\circ\text{C}$ . Further, as in the case of **2a** and **2b**, these zwitterionic species were found to be thermally robust in solution for extended periods of time at elevated temperatures.

### 3.5. Ziegler-Natta polymerization activity of **2** and **3** with ethylene and 1-hexene

With both the cationic methallyl complexes **2** and the zwitterionic allyl complexes **3** having been prepared, it was of interest to determine whether they could serve as well defined initiators for the Ziegler-Natta polymerization of ethylene and  $\alpha$ -olefins. Given the general insolubility of **2** and **3** in any solvent other than chlorobenzene, polymerization studies were limited to this solvent medium. Surprisingly, a series of studies revealed that **2** and **3** are both inactive for polymeriza-

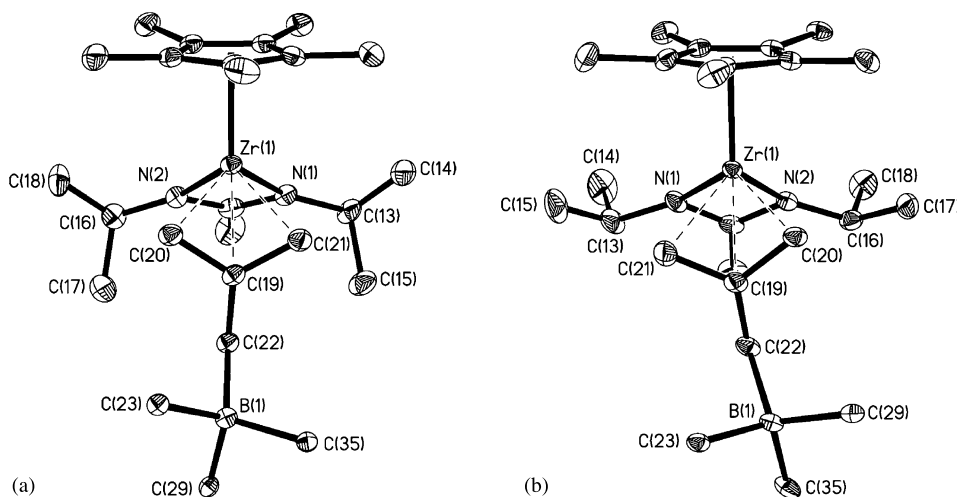


Fig. 5. Comparison of the molecular structures (30% thermal ellipsoids) of **3a** obtained from the (a) monoclinic  $C2/c$  and (b) triclinic  $P\bar{1}$  crystalline modifications. Hydrogen atoms and the aryl ring carbon and fluorine atoms of the  $B(C_6F_5)_3$  group have been removed for the sake of clarity.

tion in this solvent over a range of pressure and temperature, including a  $^1\text{H}$  NMR study that further showed that even a single insertion of 1-hexene into **2** and **3** does not occur at temperatures up to 60 °C. Upon inspection of space-filling models, the reluctance of **2** and **3** to engage in olefin insertion maybe largely steric in nature. Indeed, past observations made by us have shown that subtle differences in steric interactions can have a profound effect on the polymerization activity of the even more open  $[\text{Cp}^*\text{ZrMe}\{\text{N}(\text{R}^1)\text{C}(\text{Me})\text{N}(\text{R}^2)\}]^+[\text{B}(\text{C}_6\text{F}_5)_4]^-$  initiators [6]. The present study then serves to indicate that the formation of cationic allyl complexes from the propagating species derived from these initiators during polymerization, if it ever occurs, would be an irreversible terminating event.

#### 4. Supplementary material

Crystallographic (excluding structure factors) for the structures in this paper have been deposited with the Cambridge Crystallographic Data Centre as supplementary publication nos. CCDC 205019 (for compound **1a**), 205020 (for compound **1b**), 207303 (for compound **2b**), 205523 (for compound **3a** in the C2/2 crystalline modification) and 205524 (for compound **3a** in the  $P\bar{1}$  crystalline modification). Copies of this data can be obtained free of charge on application to The Director, CCDC, 12 Union Road, Cambridge CB2 1EZ, UK (fax: +44-1223-336-033; email: deposit@ccdc.cam.ac.uk or www: <http://www.ccdc.cam.ac.uk>).

#### Acknowledgements

This work was supported by the National Science Foundation (CHM-0092493) for which we are grateful.

#### References

- [1] (a) G. Jeske, H. Lauke, L.E. Schock, P.N. Swebstone, H. Schumann, T.J. Marks, *J. Am. Chem. Soc.* 107 (1985) 8103;
- (b) G. Jeske, H. Lauke, H. Mauermann, P.N. Swebstone, H. Schumann, T.J. Marks, *J. Am. Chem. Soc.* 107 (1985) 8091;
- (c) J.J. Eshuis, Y.Y. Tan, A. Meetsma, J.H. Teuben, J. Renkema, G.G. Evens, *Organometallics* 11 (1992) 362;
- (d) D.E. Richardson, G.N. Alameddin, M.F. Ryan, T. Hayes, J.R. Eyler, A.R. Siedle, *J. Am. Chem. Soc.* 118 (1996) 11244;
- (e) G.J. Pindando, M. Thornton-Pett, M. Bouwkamp, A. Meetsma, B. Hessen, M. Bochmann, *Angew. Chem. Int. Ed.* 37 (1997) 22358;
- (f) D. Feichtinger, D.A. Plattner, P. Chen, *J. Am. Chem. Soc.* 120 (1998) 7125;
- (g) A. Guyot, R. Spitz, J.P. Dassaud, C. Gomez, *J. Mol. Catal.* 82 (1993) 29.
- [2] L. Resconi, I. Camurati, O. Sudmeijer, *Top. Catal.* 7 (1999) 145.
- [3] (a) V. Busico, R. Cipullo, *J. Am. Chem. Soc.* 116 (1994) 9329;
- (b) M.K. Leclerc, H.H. Brintzinger, *J. Am. Chem. Soc.* 117 (1995) 1651;
- (c) M.K. Leclerc, H.H. Brintzinger, *J. Am. Chem. Soc.* 118 (1996) 9024;
- (d) J.C. Yoder, J.E. Bercaw, *J. Am. Chem. Soc.* 124 (2002) 2548.
- [4] S. Lieber, M.H. Prosenc, H.H. Brintzinger, *Organometallics* 19 (2000) 377.
- [5] (a) B. Temme, G. Erker, J. Karl, H. Luftmann, R. Fröhlich, S. Kotila, *Angew. Chem. Int. Ed.* 34 (1995) 1755;
- (b) J. Karl, G. Erker, R. Fröhlich, *J. Organometal. Chem.* 535 (1997) 59.
- [6] (a) K.C. Jayaratne, L.R. Sita, *J. Am. Chem. Soc.* 122 (2000) 958;
- (b) K.C. Jayaratne, R.J. Keaton, D.A. Henningsen, L.R. Sita, *J. Am. Chem. Soc.* 122 (2000) 10490;
- (c) R.J. Keaton, K.C. Jayaratne, J.C. Fettinger, L.R. Sita, *J. Am. Chem. Soc.* 122 (2000) 12909;
- (d) R.J. Keaton, K.C. Jayaratne, D.A. Henningsen, L.A. Koterwas, L.R. Sita, *J. Am. Chem. Soc.* 123 (2001) 6197;
- (e) K.C. Jayaratne, L.R. Sita, *J. Am. Chem. Soc.* 123 (2001) 10754;
- (f) D.A. Kissounko, J.C. Fettinger, L.R. Sita, *Inorg. Chim. Acta* 345 (2003) 121.
- [7] R.J. Keaton, L.A. Koterwas, J.C. Fettinger, L.R. Sita, *J. Am. Chem. Soc.* 124 (2002) 5932.
- [8] R.J. Keaton, L.R. Sita, *Organometallics* 21 (2002) 4315.
- [9] A.M.M. Simmons, N.S. Mills, S.R. Iyer, *Inorg. Chim. Acta* 116 (1986) 43.
- [10] (a) J.M. Mayer, C.J. Curtis, J.E. Bercaw, *J. Am. Chem. Soc.* 105 (1983) 2651;
- (b) G.C. Bazan, G. Rodriguez, B.P. Cleary, *J. Am. Chem. Soc.* 116 (1994) 2177;
- (c) G.E. Herberich, C. Kreuden, U. Englert, *Angew. Chem. Int. Ed.* 33 (1994) 2465.
- [11] (a) S. Braun, H.O. Kalinowski, S. Berger, 100 and More Basic NMR Experiments, VCH Publishers, New York, 1996;
- (b) C.L. Perrin, T.J. Dwyer, *Chem. Rev.* 90 (1990) 935.